

# PCCP

Accepted Manuscript



This article can be cited before page numbers have been issued, to do this please use: N. Jian, K. Qu, H. Gu, L. Zou, X. Liu, F. Hu, J. Xu, Y. Yu and B. Lu, *Phys. Chem. Chem. Phys.*, 2019, DOI: 10.1039/C9CP00672A.



This is an Accepted Manuscript, which has been through the Royal Society of Chemistry peer review process and has been accepted for publication.

Accepted Manuscripts are published online shortly after acceptance, before technical editing, formatting and proof reading. Using this free service, authors can make their results available to the community, in citable form, before we publish the edited article. We will replace this Accepted Manuscript with the edited and formatted Advance Article as soon as it is available.

You can find more information about Accepted Manuscripts in the [author guidelines](#).

Please note that technical editing may introduce minor changes to the text and/or graphics, which may alter content. The journal's standard [Terms & Conditions](#) and the ethical guidelines, outlined in our [author and reviewer resource centre](#), still apply. In no event shall the Royal Society of Chemistry be held responsible for any errors or omissions in this Accepted Manuscript or any consequences arising from the use of any information it contains.

## Highly fluorescent triazolopyridine-thiophene D-A-D oligomers for efficient pH sensing in both solution and solid state

Nannan Jian<sup>a</sup>, Kai Qu<sup>a</sup>, Hua Gu<sup>b</sup>, Lie Zou<sup>b</sup>, Ximei Liu<sup>b</sup>, Faqi Hu<sup>b</sup>, Jingkun Xu<sup>\*a,b</sup>, Yan Yu<sup>\*c</sup>, Baoyang Lu<sup>\*a,b</sup>

Received 00th January 20xx,  
Accepted 00th January 20xx

DOI: 10.1039/x0xx00000x

[www.rsc.org/](http://www.rsc.org/)

Conjugated fluorophores have been extensively used for fluorescent sensing of various substances in the field of life processes as well as environmental science, due to their noninvasiveness, sensitivity, simplicity and rapidity. Most existing conjugated fluorophores exhibit excellent light-emitting performances in dilute solutions, but their properties substantially decrease or even completely vanish due to severe aggregation quenching in solid state. Herein, we synthesize a series of triazolopyridine-thiophene donor-acceptor-donor (D-A-D) type conjugated molecules with high absolute fluorescence quantum yields ( $\Phi_f$ ) ranging from 80% to 89% in solution. These molecules also show unusual light-emitting nature in solid state with  $\Phi_f$  up to 26%. We find that owing to the protonation-deprotonation process of the pyridine ring, these compounds display obvious fluorescence changes in both wavelength and intensity upon addition of acids, and these changes can be readily recovered by successive introduction of bases. By harnessing this phenomenon, we further show that these fluorophores can be employed for efficient and reversible fluorescence sensing of hydrogen ions in a broad pH range (0.0 ~ 7.0). With the fabrication of pH testing papers and ink-printed complex patterns including butterflies and letters on substrate, we demonstrate the applications of such sensors towards fluorescence indicating or solid state pH detection for real samples such as volatile acidic/basic gas and water-quality analysis.

### Introduction

Push-pull conjugated fluorophores and related polymeric systems, also known as donor-acceptor-donor (D-A-D) type conjugated systems, are an important class of fluorescence and light emitting materials that have been extensively studied and utilized in various technologies.<sup>1-12</sup> Their molecular structures generally contain electron rich (donor) and electron deficient (acceptor) moieties linked via a  $\pi$ -conjugated bridge. Photoexcitation leads to the intramolecular charge-transfer from the electron rich units in the molecule to the electron deficient fragments.<sup>13</sup> Such a redistribution of electron density usually leads to extended absorption/emission bands all the way from the ultraviolet to the near-infrared regions, depending on the electronic offset between the donor and acceptor components and the overall delocalization length.<sup>14</sup> This type of materials usually exhibit excellent photophysical properties, sensitivity, simplicity, rapidity and noninvasiveness, and have been utilized in many organic electronic and optical applications including use as fluorescent indicating and

sensing,<sup>15</sup> nonlinear optics,<sup>16</sup> as light emitters for OLEDs,<sup>17</sup> and as light harvesting materials for solar cells.<sup>18</sup>

Although much progress has been made on conjugated fluorophores in terms of both materials development and practical applications,<sup>19,20</sup> most existing conjugated fluorophores exhibit relatively high absolute  $\Phi_f$  and excellent photostability in dilute solutions,<sup>21-23</sup> whereas their light-emitting properties substantially decrease or even completely vanish in the solid state due to the strong intermolecular  $\pi$ - $\pi$  stacking interactions.<sup>24,25</sup> Up to date, rational design of novel conjugated D-A-D fluorophores with high performances in both solution and solid state is still significant to this field in terms of various practical application requirements.

The most common yet effective strategy to design new D-A-D molecules with tunable optical and electronic properties is to modify the electron donating and/or accepting nature of the D or A fragments, respectively. Most recently, we and other groups developed a new type of acceptor moieties, chalcogenodiazolo[3,4-c]pyridine and their analogues/derivatives, which have been successfully employed towards rational design of narrow band gap D-A-D polymers with high performance in organic electronics.<sup>26-31</sup> It was also found that those D-A-D type polymers also display excellent fluorescence in organic solution and can be utilized for fluorescent sensing towards proton and even Lewis acids.<sup>26,27,29</sup> However, like most reported D-A-D type molecular systems, chalcogenodiazolo[3,4-c]pyridine-based conjugated fluorophores display significantly decreased or even

<sup>a</sup> School of Chemistry & Chemical Engineering, Jiangxi Science & Technology Normal University, Nanchang 330013, Jiangxi, PR China;

<sup>b</sup> School of Pharmacy, Jiangxi Science & Technology Normal University, Nanchang 330013, Jiangxi, PR China;

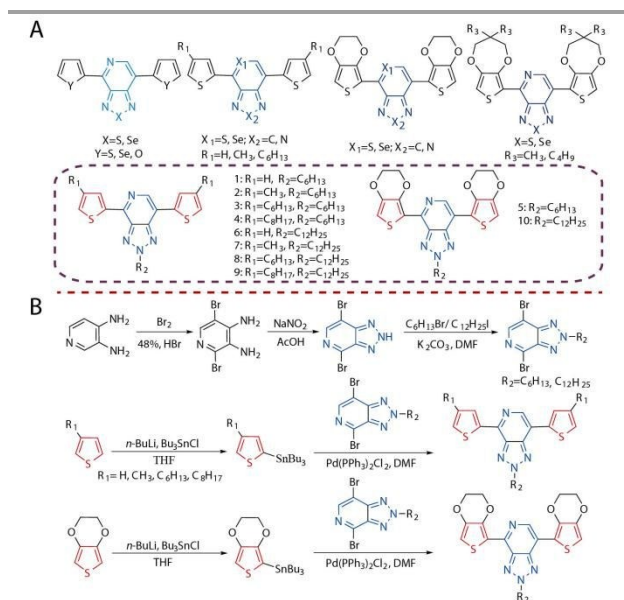
<sup>c</sup> School of Optical and Electronic Information, Huazhong University of Science and Technology, Wuhan 430074, Hubei, PR China.

\*Corresponding author. Email: [lby1258@163.com](mailto:lby1258@163.com); [xujingkun1971@yeah.net](mailto:xujingkun1971@yeah.net); and [yuyan19840218@hust.edu.cn](mailto:yuyan19840218@hust.edu.cn)

completely disappeared light-emitting in solid state compared to their corresponding diluted solution due to aggregation-caused fluorescence quenching during the solid state packing.

From the materials development perspective, conjugated fluorophores based on triazolo[4,5-c]pyridine (PTz), an important nitrogen analogue of chalcogenodiazolo[3,4-c]pyridine which can be facilely modified on the N position with different functional groups might reveal excellent fluorescence and sensing properties in both solution and solid state, due to the feasibility of reducing the strong intermolecular  $\pi$ - $\pi$  stacking interactions. Furthermore, the protonation-deprotonation of pyridine ring allow these compounds to serve as fluorescence sensing materials for effective detection of acids like pH. Unfortunately, to the best of our knowledge, rational design and structure-property relationship of triazolo[4,5-c]pyridine-based D-A-D molecular systems have not been well known and explored for fluorescent chemosensors.

Here, based on the 2H-[1,2,3]triazolo[4,5-c]pyridine (PTz) moiety, we design and synthesize a series of novel triazolopyridine-thiophene D-A-D type conjugated fluorophores (1~10, **Scheme 1**) with alkyl substitution to enhance the solubility and solid-state fluorescence. Systematic investigation of their structure-property relationship as well as photophysical properties demonstrates excellent fluorescence properties of these D-A-D molecular systems both in the diluted solutions and solid state. Moreover, efficient and reversible pH sensing behavior in both solution and solids are observed for these molecules. Enabled by their good solubility, we further demonstrate the facile fabrication of complex patterns by ink-jet printing such as butterflies and letters, and explore their potential applications for the detection of volatile acidic/basic vapor.



**Scheme 1** (A) Chemical structures of typical chalcogenodiazolo[3,4-c]pyridine derivatives-based conjugated D-A-D type molecules reported in literature and triazolopyridine-thiophene systems synthesized in this work. (B) Detailed synthetic routes of triazolopyridine-thiophene D-A-D type molecules 1 ~ 10 via Stille coupling.

## Experimental

### 2.1 Materials

Building blocks like thiophene (Th, 99.5%, Sigma-Aldrich), 3-methylthiophene (3MT, 98%, Sigma-Aldrich), 3-hexylthiophene (3HT, 99%, Sigma-Aldrich), 3-octylthiophene (3OT, 97%, Sigma-Aldrich), and 3,4-ethylenedioxythiophene (EDOT, 97%, J&K) were all used as received. Other reagents were purchased from guaranteed chemical plants and directly used for the synthetic procedure, such as *n*-butyllithium (*n*-BuLi, 1.6 mol L<sup>-1</sup> in hexanes, J&K), chlorotributyltin (SnBu<sub>3</sub>Cl, J&K), acetic acid (AcOH, 99%, J&K), sodium nitrite (NaNO<sub>2</sub>, ≥ 99.999% trace metals basis; 98-102% (RT), Sigma-Aldrich), triethylamine (99.5%, Energy), 1-bromohexane (99%, Shanghai Vita), 1-iodododecane (98%, stabilized with copper, Shanghai Vita), dichloromethane (DCM, 99.9%, superdry, with molecular sieves, J&K), acetonitrile (ACN, 99.9%, ACS/HPLC certified, J&K). Tetrahydrofuran (THF), as solvent for stannylation, was purified by distillation with sodium under nitrogen atmosphere before use. Trans-dichlorobis(triphenyl-phosphine)palladium (II) (Pd(PPh<sub>3</sub>)<sub>2</sub>Cl<sub>2</sub>, 98%, 15% Pd, Sigma-Aldrich) was employed as the catalyst for Stille coupling. Tetrabutylammonium hexafluorophosphate (TBAPF<sub>6</sub>, 99%, Shanghai Vita), electrolyte for the electrochemical polymerization, was dried under vacuum at 60 °C for 24 h before use.

### 2.2 Instruments and characterization

A Bruker AV 400 NMR spectrometer was employed for <sup>1</sup>H and <sup>13</sup>C NMR spectral measurements, with trimethylsilane (TMS) as the internal standard and CDCl<sub>3</sub> or DMSO-*d*<sub>6</sub> as the solvent. A X-4 digital display micro melting point instrument was used to determine the melting points of triazolopyridine-thiophene D-A-D type conjugated fluorophores. Infrared spectra were performed with a Bruke Vertex 70 Fourier-transform infrared (FT-IR) spectrometer. The electronic spectra were recorded on a Lambda 750 UV-Vis spectrophotometer. Theoretical calculations of all triazolopyridine-thiophene D-A-D type fluorophores were performed by DFT methods with the Gaussian 09 program package. Becke's three-parameter gradient corrected functional (B3LYP) with the 6-31G (d,p) basis in vacuum was used for all the compounds to optimize the structure geometry and to compute the electronic structures at the minimum found. Electrochemical polymerization was investigated by a Versa Stat 3 electrochemical workstation (EG&G Princeton Applied Research). Pt wires (diameter: 1 mm) were employed as the working and counter electrodes, and an Ag/AgCl electrode as the reference electrode, respectively. Moreover, in order to minimize the oxygen effect, the electrolytic system was bubbled by nitrogen stream before experiments. In order to obtain sufficient polymers for further characterization, Pt sheet (2×1.5 cm<sup>2</sup>) was used as working electrode and another Pt sheet (2×2 cm<sup>2</sup>) was employed as the counter electrode.

### 2.3 Synthesis

**Scheme 1** illustrates the synthetic route of various triazolopyridine-thiophene D-A-D type conjugated fluorophores. Hexyl and dodecyl substituted

[1,2,3]triazolo[4,5-c]pyridine (HPTz and DPTz) were chosen as the acceptors, while thiophenes like Th, 3MT, 3HT, 3OT and EDOT were employed as the donors, and all these molecular systems were synthesized by Stille coupling. Stannylation of thiophenes occurred at 2-position with tri-*n*-butyltin chloride, and they were employed for the next step immediately without further purification.<sup>32-35</sup> Acceptor intermediates such as 4,7-dibromo-[1,2,3] triazolo[4,5-c]pyridine, 4,7-dibromohexyl[1,2,3]triazolo[4,5-c]pyridine and 4,7-dibromododecyl[1,2,3]triazolo[4,5-c]pyridine were synthesized according to previously reported procedures.<sup>36-40</sup> The primary synthetic procedures are described as following.

**4,7-Dibromo-[1,2,3]triazolo[4,5-c]pyridine.** To a solution of 2,5-dibromopyridine-3,4-diamine (0.80 g, 3.00 mmol) in acetic acid (12.00 mL, AcOH), a solution of NaNO<sub>2</sub> (0.30 g, 3.30 mmol) in deionized water (6.00 mL) was gradually added at room temperature. The mixture was stirred for 20 min at the same temperature. Then, the precipitate was obtained by filtration and washed with deionized water. The crude products were directly used for the next step without further purification.

**4,7-Dibromo-hexyl[1,2,3]triazolo[4,5-c]pyridine and 4,7-dibromo-dodecyl[1,2,3]triazolo[4,5-c]pyridine.** A solution of 4,7-dibromo-[1,2,3]triazolo[4,5-c]pyridine (0.61 g, 2.20 mmol) in *N,N*-dimethylformamide (DMF, 30.00 mL), triethylamine (2.50 mmol) was slowly added under nitrogen atmosphere. After stirring for 1 h, 1-bromohexane (0.41 g, 2.50 mmol)/1-iodododecane (0.74 g, 2.50 mmol) were added drop-wise. The reaction was stirred for 24 h at room temperature. DMF was removed, while organic layer was extracted with DCM and then purified by silica column chromatography.

**4,7-Dibromo-hexyl[1,2,3]triazolo[4,5-c]pyridine.** 70% yield. <sup>1</sup>H NMR (400 MHz, CDCl<sub>3</sub>, ppm): 8.34 (s, 1H), 4.82 (t, J = 7.40 Hz, 2H), 2.25~2.10 (m, 2H), 1.45~1.31 (m, 6H), 0.88 (dd, J = 8.60, 5.20 Hz, 3H).

**4,7-Dibromo-dodecyl[1,2,3]triazolo[4,5-c]pyridine.** 73% yield. <sup>1</sup>H NMR (400 MHz, CDCl<sub>3</sub>, ppm): 8.34 (s, 1H), 4.82 (t, J = 7.40 Hz, 2H), 2.16 (d, J = 7.30 Hz, 2H), 1.39~1.24 (m, 17H), 0.89 (dd, J = 15.0, 8.30 Hz, 4H).

**Representative procedures for the synthesis of 1~10.** To a solution of stannyliated donors (10.00 mmol) and 4,7-dibromohexyl[1,2,3]triazolo[4,5-c]pyridine (0.72 g, 2.00 mmol) or 4,7-dibromo-dodecyl[1,2,3]triazolo[4,5-c]pyridine (0.89 g, 2.00 mmol) in DMF (30.00 mL), trans-dichlorobis(triphenylphosphine)palladium (II) (Pd(PPh<sub>3</sub>)<sub>2</sub>Cl<sub>2</sub>, 0.14 g, 0.20 mmol) was added, and then the mixture was stirred for 24 h at 110 °C. After the reaction, the mixture was poured into deionized water and extracted with DCM. The organic layer was purified by silica column chromatography.

**Th-HPTz (1).** 76% yield. <sup>1</sup>H NMR (400 MHz, DMSO-*d*<sub>6</sub>, ppm): 8.76 (s, 1H), 8.44 (s, 1H), 8.09 (s, 1H), 7.86 (s, 1H), 7.76 (s, 1H), 7.43~7.22 (m, 2H), 4.96 (t, J = 7.00 Hz, 2H), 2.23~2.05 (m, 2H), 1.32 (dd, J = 15.7, 8.60 Hz, 6H), 0.87 (d, J = 6.40 Hz, 3H). <sup>13</sup>C NMR (400 MHz, CDCl<sub>3</sub>, ppm): 155.82, 144.46, 143.34, 142.46, 141.41, 132.05, 131.64, 130.27, 130.02, 128.32, 127.88, 127.46, 126.98, 59.73, 39.90, 39.79, 22.77, 22.58, 16.91. FT-IR (ATR, cm<sup>-1</sup>): 3085, 2831, 2847, 1587, 1550, 1491, 1362, 1201, 1150, 1071, 711.

**3MT-HPTz (2).** 94% yield. <sup>1</sup>H NMR (400 MHz, CDCl<sub>3</sub>, ppm): 8.63 (s, 1H), 8.30 (s, 1H), 7.84 (s, 1H), 7.12 (s, 1H), 6.98 (s, 1H), 4.86 (t, J = 7.20 Hz, 2H), 2.37 (d, J = 9.10 Hz, 6H), 2.21 (dd, J = 14.1, 7.10 Hz, 2H), 1.35 (d, J = 7.60 Hz, 6H), 0.97 (d, J = 6.60 Hz, 3H). <sup>13</sup>C NMR (400 MHz, CDCl<sub>3</sub>, ppm): 153.16, 144.04, 140.89, 138.53, 138.11, 137.64, 137.53, 136.09, 131.58, 129.01, 124.22, 123.97, 120.89, 117.42, 56.59, 30.48, 29.39, 25.55, 21.80, 16.67, 15.20. FT-IR (ATR, cm<sup>-1</sup>): 3087, 2927, 2553, 1579, 1552, 1489, 1365, 1195, 1151, 1072, 713.

**3HT-HPTz (3).** 84% yield. <sup>1</sup>H NMR (400 MHz, CDCl<sub>3</sub>, ppm): 8.64 (s, 1H), 8.30 (s, 1H), 7.85 (s, 1H), 7.13 (s, 1H), 7.00 (s, 1H), 4.87 (t, J = 7.00 Hz, 2H), 2.70 (dd, J = 15.8, 8.00 Hz, 4H), 2.23~2.10 (m, 2H), 1.76~1.67 (m, 4H), 1.38~1.33 (m, 13H), 0.94~0.90 (m, 14H). <sup>13</sup>C NMR (400 MHz, CDCl<sub>3</sub>, ppm): 154.24, 144.69, 141.54, 139.18, 138.76, 138.29, 129.66, 127.44, 124.87, 121.54, 118.07, 57.24, 32.25, 31.13, 30.04, 28.22, 26.77, 26.20, 24.42, 23.34, 22.45, 13.97. FT-IR (ATR, cm<sup>-1</sup>): 3080, 2934, 2854, 1581, 1549, 1493, 1368, 1221, 1154, 1058, 698.

**3OT-HPTz (4).** 69% yield. <sup>1</sup>H NMR (400 MHz, DMSO-*d*<sub>6</sub>, ppm): 8.68 (s, 1H), 8.27 (s, 1H), 7.94 (s, 1H), 7.46 (s, 1H), 7.35 (s, 1H), 4.96 (t, J = 6.90 Hz, 2H), 2.66 (dd, J = 15.7, 8.00 Hz, 4H), 2.16~2.08 (m, 2H), 1.64 (s, 4H), 1.37~1.23 (m, 24H), 0.86 (dd, J = 15.4, 8.10 Hz, 10H). <sup>13</sup>C NMR (400 MHz, CDCl<sub>3</sub>, ppm): 154.09, 144.54, 141.39, 139.03, 138.61, 138.14, 129.51, 127.29, 124.72, 121.39, 117.92, 57.09, 33.73, 30.98, 29.89, 28.07, 26.62, 26.05, 24.27, 23.19, 22.30, 13.82. FT-IR (ATR, cm<sup>-1</sup>): 3091, 2930, 2849, 1582, 1547, 1492, 1360, 1204, 1150, 1056, 697.

**EDOT-HPTz (5).** 91% yield. <sup>1</sup>H NMR (400 MHz, CDCl<sub>3</sub>, ppm): 9.38 (s, 1H), 6.72 (s, 1H), 6.56 (s, 1H), 4.86 (t, J = 7.20 Hz, 2H), 4.57 (s, 2H), 4.45~4.26 (m, 6H), 2.19 (dd, J = 14.4, 7.20 Hz, 2H), 1.43~1.32 (m, 6H), 0.90 (dd, J = 7.20, 3.80 Hz, 3H). <sup>13</sup>C NMR (400 MHz, CDCl<sub>3</sub>, ppm): 155.34, 152.57, 151.77, 145.42, 144.71, 114.78, 113.85, 95.42, 94.88, 66.09, 65.07, 64.45, 63.88, 57.27, 31.15, 30.06, 26.79, 26.22, 15.98. FT-IR (ATR, cm<sup>-1</sup>): 3088, 2926, 2852, 1580, 1548, 1495, 1364, 1197, 1155, 1070, 701.

**Th-DPTz (6).** 72% yield. <sup>1</sup>H NMR (400 MHz, DMSO-*d*<sub>6</sub>, ppm): 8.75 (s, 1H), 8.43 (d, J = 3.60 Hz, 1H), 8.09 (d, J = 3.50 Hz, 1H), 7.85 (d, J = 5.00 Hz, 1H), 7.75 (d, J = 5.00 Hz, 1H), 7.36~7.24 (m, 2H), 4.94 (t, J = 6.80 Hz, 2H), 2.19~2.05 (m, 2H), 1.19 (d, J = 24.0 Hz, 17H), 0.87 (d, J = 7.30 Hz, 4H). <sup>13</sup>C NMR (400 MHz, CDCl<sub>3</sub>, ppm): 150.91, 149.44, 143.34, 142.36, 130.44, 130.27, 130.02, 129.68, 129.38, 129.09, 128.94, 128.65, 61.27, 32.20, 31.00, 30.00, 29.36, 28.29, 27.75, 27.08, 26.54, 26.05, 22.77, 22.58, 17.49. FT-IR (ATR, cm<sup>-1</sup>): 3092, 2820, 2846, 1581, 1550, 1491, 1369, 1195, 1147, 1067, 705.

**3MT-DPTz (7).** 74% yield. <sup>1</sup>H NMR (400 MHz, CDCl<sub>3</sub>, ppm): 8.63 (s, 1H), 8.33 (s, 1H), 7.84 (s, 1H), 7.14 (s, 1H), 6.99 (s, 1H), 4.87 (t, J = 7.20 Hz, 2H), 2.38 (d, J = 9.60 Hz, 6H), 2.25~2.17 (m, 2H), 1.47~1.32 (m, 17H), 0.98~0.94 (m, 4H). <sup>13</sup>C NMR (400 MHz, CDCl<sub>3</sub>, ppm): 154.05, 144.77, 141.63, 139.27, 138.85, 138.38, 138.27, 136.82, 132.32, 129.75, 124.95, 124.70, 121.63, 118.16, 57.33, 45.83, 40.50, 40.32, 31.22, 30.13, 26.86, 22.54, 17.41, 15.94, 14.06, 13.67. FT-IR (ATR, cm<sup>-1</sup>): 3088, 2934, 2825, 1580, 1557, 1493, 1368, 1195, 1153, 1062, 695.

**3Hh-DPTz (8).** 64% yield. <sup>1</sup>H NMR (400 MHz, CDCl<sub>3</sub>, ppm): 8.64 (s, 1H), 8.32 (s, 1H), 7.86 (s, 1H), 7.15 (s, 1H), 7.01 (s, 1H), 4.87 (t, J = 7.00 Hz, 2H), 2.70 (dd, J = 15.8, 8.00 Hz, 4H), 2.28~2.15

(m, 2H), 1.70 (m, 4H), 1.39~1.22 (m, 29H), 0.92~0.85 (m, 10H). <sup>13</sup>C NMR (400 MHz, CDCl<sub>3</sub>, ppm): 153.82, 144.27, 141.12, 138.76, 138.34, 137.87, 129.24, 127.02, 124.45, 121.12, 117.65, 56.82, 32.25, 30.71, 30.03, 29.62, 28.65, 27.80, 27.08, 26.35, 25.78, 24.88, 24.00, 22.03, 21.28, 20.13, 15.54. FT-IR (ATR, cm<sup>-1</sup>): 3087, 2921, 2845, 1584, 1557, 1492, 1367, 1195, 1158, 1059, 691.

**3OT-DPTz (9)**. 56% yield. <sup>1</sup>H NMR (400 MHz, DMSO-*d*<sub>6</sub>, ppm): 8.68 (s, 1H), 8.27 (s, 1H), 7.95 (s, 1H), 7.46 (s, 1H), 7.35 (s, 1H), 4.96 (s, 2H), 2.66 (d, *J* = 8.20 Hz, 4H), 2.13 (s, 2H), 1.59 (d, *J* = 7.70 Hz, 6H), 1.41~1.13 (m, 35H), 0.90~0.84 (m, 10H). <sup>13</sup>C NMR (400 MHz, CDCl<sub>3</sub>, ppm): 154.25, 144.70, 141.55, 139.20, 138.78, 138.31, 129.68, 127.46, 124.89, 121.56, 118.08, 57.26, 33.90, 32.68, 31.15, 30.05, 29.08, 28.23, 26.79, 26.21, 24.43, 22.46, 17.33, 15.97, 14.98, 13.98, 13.60. FT-IR (ATR, cm<sup>-1</sup>): 3089, 2922, 2848, 1585, 1552, 1492, 1362, 1197, 1159, 1057, 701.

**EDOT-DPTz (10)**. 85% yield. <sup>1</sup>H NMR (400 MHz, CDCl<sub>3</sub>, ppm): 9.55 (s, 1H), 6.87 (s, 1H), 6.61 (s, 1H), 4.89 (t, *J* = 6.90 Hz, 2H), 4.70 (s, 2H), 4.48~4.22 (m, 6H), 2.21 (d, *J* = 7.70 Hz, 2H), 1.24 (s, 17H), 0.87 (t, *J* = 6.80 Hz, 4H). <sup>13</sup>C NMR (400 MHz, CDCl<sub>3</sub>, ppm): 155.19, 152.42, 151.62, 145.27, 144.56, 114.63, 113.70, 95.27, 94.73, 65.94, 64.92, 64.30, 63.73, 57.12, 31.80, 31.01, 29.91, 28.09, 26.65, 26.07, 25.17, 24.29, 23.22, 22.32, 15.83. FT-IR (ATR, cm<sup>-1</sup>): 3087, 2929, 2850, 1579, 1549, 1490, 1360, 1198, 1152, 1069, 703.

#### 2.4 Detection of fluorescence sensing

A series of aqueous solutions with different pH from 0.00 to 7.00 were prepared with HCl and deionized water, and the pH values were confirmed by using a pH meter. Typically, the stock standard solutions (40 μL, 15 μM) of fluorophores dissolving in DMSO were added to different pH solutions (2 mL). After 10 min of equilibration time, the fluorescence spectra were recorded with an F-4500 fluorescence spectrophotometer with excitation and emission slit set at 5 nm.

#### 2.5 The preparation of pH test papers and patterning

The fluorescence pH testing papers were prepared by dipping filter paper into a DCM solution of fluorophores (0.1 mg in 1 mL DCM) for 10 s. Then, these test papers were dried in air for

24 h in dark at room temperature. Fluorescent detection of volatile acid/base vapor was conducted using a culture dish. Patterning of the fluorescent butterfly and letters were fabricated by inkjet-printing of these fluorophores dissolving into DCM on substrates using a Canon MG3620 printer.

## Results and Discussion

### 3.1 Molecular design and synthesis

From the molecular design perspective, the combination of donors and acceptors can effectively tune the photophysical properties of molecules. Alkyl substituted donors/acceptors have been introduced into the π-conjugated systems to increase solution processability and weaken intermolecular π-π stacking interactions. A series of novel triazolopyridine-thiophene D-A-D type conjugated fluorophores (**1** ~ **10**) are synthesized via Stille coupling (**Scheme 1**). All intermediates and target fluorophores are obtained in relatively high yields (typically over 70%). Their molecular structures are all determined by NMR spectra (**Fig. S1** ~ **Fig. S22**) and FT-IR spectra (**Fig. S23** and **Table S1**).

Density functional theory (DFT) calculations were used to study the conformational and electronic properties of triazolopyridine-thiophene D-A-D type conjugated fluorophores (**1** ~ **10**). DFT calculations are beneficial for confirming molecular geometry, predicting optimized molecular structures and electronic energy levels, and demonstrating complete delocalization across the molecular backbones.<sup>41-44</sup> From the theoretical calculations (**Table 1** and **Table S2**), the optimized geometries of all the triazolopyridine-based D-A-D type fluorophores shows quasi-planar conjugated systems with small dihedral twist angles between each block. The molecular orbital distribution results suggest that the LUMO is mostly localized on the triazolopyridine acceptor unit, whereas the HOMO is well-distributed over the entire molecular structure, and the energy levels vary with the electron-donating ability of the end-capping moieties. This is in good agreement with most reported calculations of D-A-D type

**Table 1** Optical parameters and DFT theoretical calculation data of triazolopyridine-thiophene D-A-D type conjugated fluorophores (1~10).

Fluorophores	HOMO <sub>DFT</sub> (eV)	LUMO <sub>DFT</sub> (eV)	Dihedral angles(°)	E <sub>g,opt</sub> (eV)	λ <sub>max,1</sub> (nm)	λ <sub>max,2</sub> (nm)	λ <sub>max,3</sub> (nm)	λ <sub>em</sub> (nm)	Φ <sub>F</sub> [%]	
									solution	solid
1	-5.27	-2.09	14.0, 0.10	2.79	242	276	397	498	86.7	25.2
2	-5.19	-2.03	13.9, 0.37	2.70	240	278	407	508	87.8	15.1
3	-5.17	-2.02	16.5, 0.56	2.74	238	281	408	509	87.8	24.7
4	-5.15	-2.03	6.96, 0.53	2.72	239	282	408	509	89.2	26.0
5	-4.83	-1.78	4.07, 3.76	2.58	248	292	417	520	82.5	14.6
6	-5.27	-2.08	15.2, 0.49	2.83	243	277	400	498	86.9	23.2
7	-5.19	-2.03	14.8, 0.08	2.70	238	281	408	510	86.5	18.6
8	-5.15	-2.02	8.88, -0.42	2.74	238	281	409	510	88.1	22.9
9	-5.17	-2.01	14.6, -0.43	2.72	240	281	410	510	88.6	20.2
10	-4.82	-1.77	5.05, 3.94	2.63	246	294	418	521	79.8	13.2

molecule systems.<sup>45-47</sup> Note here that triazolopyridine-based D-A-D type fluorophores exhibited slightly higher LUMO than their chalcogenodiazolo[3,4-c]pyridine analogs (Table S3). This phenomenon is mainly caused by the introduction of long alkyl chain spacers on triazolopyridine acceptor, which interrupts the intermolecular arrangement of these systems.

### 3.2 Photophysical properties

Owing to the introduction of long alkyl chains, these D-A-D type fluorophores indeed reveal excellent solubility in common organic solvents, for instance, dimethyl sulfoxide (DMSO), acetonitrile (ACN), tetrahydrofuran (THF), DCM, and chloroform (CDCl<sub>3</sub>). The superior solubility of these fluorophores can facilitate their practical applications in various fields. As typical D-A-D type systems, all these triazolopyridine-thiophene molecules reveal characteristic dual-band absorptions in the UV-vis spectra (Fig. 1A and Fig. S24). To be specific, the  $\pi$ - $\pi^*$  transition (both E1 and K absorption bands) of individual aromatic units like thiophene ring in these conjugated systems results in two maximum peaks at short wavelengths (230~300 nm), whereas charge transfer between different donor units and acceptors as well as the n- $\pi^*$  transition of the triazolopyridine units (R bands from C=N and N=N bonds) typically yield red-shifted maximum absorption peaks extended to longer wavelengths in the range of 395~420 nm.<sup>26,27,29,48</sup> Moreover, the extension of side chains in thiophene-based donor units is found to cause slight red shifts in the absorption peaks due to the fact that side groups with varying electron-donating ability exert different changes on the electronic structures of these D-A-D type fluorophores.<sup>49,50</sup> For example, due to the extended alkyl chain reducing the LUMO level, the absorption bands of dodecyl modified triazolopyridine-based fluorophores show bathochromic shift to lower energy region compared to their hexyl analogs. Compared to our previous results of chalcogenodiazolo[3,4-c]pyridine-based analogs, the absorption bands of triazolopyridine-thiophene D-A-D type precursors slightly blue-shift to higher energy regions due to the stronger electron-deficient nature of triazolopyridine unit. (Table S3).<sup>26,27,29,51-55</sup>

Although a series of chalcogenodiazolo[3,4-c]pyridine-based D-A-D type conjugated fluorophores have been obtained in the

dilute solution (Table S3), whereas their fluorescence performances severely decrease or even completely vanish in the solid state due to aggregation-caused fluorescence quenching during the solid state packing. So far, only a few materials reveal light-emitting properties with  $\Phi_F$  greater than 20% in both solution and solid state.<sup>26</sup> Interestingly, we find that these triazolopyridine-based D-A-D type fluorophores in this work demonstrate very strong light emitting nature with outstanding  $\Phi_F$  both in dilute solution (up to 89%) and in the solid state (up to 26%) (Fig. 1A, Fig. S24, and Table 1). The emission peaks of these compounds are generally in the range of 498~521 nm (Fig. 1B, Fig. S24, and Table 1), typically in the blue (450 ~ 500 nm) to green (500 ~ 570 nm) region. In good agreement with UV-vis spectral results, the emission spectra also display slight red shifts owing to the increase of electron-donating capacity from Th to alkyl thiophenes and further to EDOT.<sup>6</sup> Overall, triazolopyridine-based D-A type fluorophores reported herein display better fluorescence properties than their chalcogenodiazolo[3,4-c]pyridine analogs (Table S3),<sup>26,27,29,51-55</sup> and even higher than most of the fluorescent materials.<sup>56-58</sup> This is mainly due to the fact that the stronger electron-deficient nature of triazolopyridine unit decreases the singlet oxygen generation efficiency and increases the emission intensity.

### 3.3. Fluorescence quenching/recovery of pH sensing

Guaranteed by their superior solubility, these fluorophores can be dissolved into many organic solvents and even water-based binary solvents such as water-DMSO, water-ACN, etc. These molecules are expected to possess good sensitivity towards hydrogen ions and even electron-deficient atoms in Lewis acids (like BF<sub>3</sub>)<sup>59</sup> due to the fact the lone pair electrons at the N position in pyridine ring. Moreover, the pH sensing performances are probably improved owing to the molecular wire magnification effect from extended  $\pi$ -conjugated molecular backbone. To examine the fluorescence sensing properties, we choose the binary solvent of water and DMSO as testing system since both water and DMSO are nontoxic and environmentally friendly. As expected, all these fluorophores reveal strong blue to green light-emission in such media, and a gradual fluorescence quenching is observed with stepwise addition of acids like HCl (Fig. 2A and Fig. S25). Meanwhile, the emitting color of the fluorophores correspondingly changes from blue or green to kelly, yellow, and further to claybank due to the protonation of pyridine ring with hydriions. Interestingly, this fluorescence quenching can be easily recovered with the addition of bases like sodium hydroxide solution (NaOH) owing to the deprotonation of nitrogen on the pyridine ring (Fig. 2A and Fig. S25), indicating a reversible coordination process between fluorophores and acids. The light-emitting color changes also imply the reversible pH detection and this process even can be easily observed by naked eyes.

Fluorescent spectroscopy is more sensitive to small changes in emission and quantitatively disclose the detailed information during the quenching and recovery process.<sup>60,61</sup> In order to further evaluate the sensing performances of these molecules,

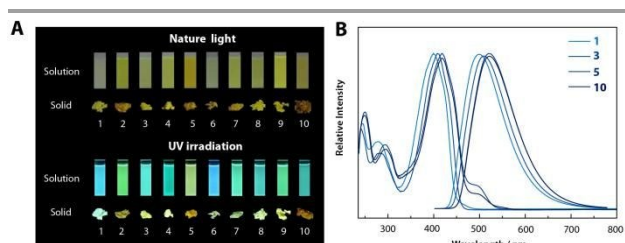


**Fig. 1** (A) Photoluminescence of triazolopyridine-thiophene D-A-D type conjugated fluorophores (1~10) in both solution (DCM) and solid state. (B) UV-Vis absorption and emission spectra of representative triazolopyridine-thiophene D-A-D type conjugated fluorophores (1, 3, 5 and 10) in DCM.

last several years,<sup>26,27,29,51-55</sup> these molecules mostly exhibit bright light-emitting properties with high  $\Phi_F$  (0.072-0.849) in

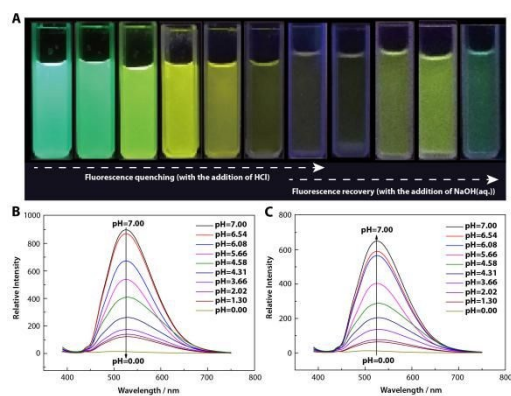


**Fig. 2** (A) Images of fluorescence quenching/recovery of triazolopyridine-thiophene D-A-D type conjugated fluorophores (exemplified by fluorophore 2) upon addition of HCl and reversed by NaOH in water-DMSO. (B) Fluorescence quenching in emission spectra of fluorophore 2 (15  $\mu$ M) against pH decrease from 7.00 to 0.00 (adjusted by addition of HCl). Excitation: 380 nm. (C) Fluorescence recovery in emission spectra of fluorophore 2-hydriens complex by adding bases (adjusted pH from 0.00 to 7.00 by NaOH). Excitation: 380 nm.

we recorded the emission spectra of these fluorophores at different pH values (Fig. 2B, Fig. S26). Clearly, the fluorescence intensity at maximum emission peak decreased gradually with decreasing the pH owing to the protonation of nitrogen atom on the pyridine ring. Such quenching of these fluorophores provides an effective method to detect hydrogen ions. The relationship between fluorescence intensity and the pH values is shown in Fig. S26. Obviously, fluorescence intensity displays a monotonical decrease against pH, revealing that this method is suitable for detecting the unknown content of pH in a broad pH range (0.0 ~ 7.0).

Reversibility will enable fluorophores to be utilized in a wider range of applications. We find that the fluorescence quenching of fluorophores against hydrogen proton can be recovered by adding bases like NaOH into the system (Fig. 2C). With the addition of bases, hydroxyl in the aqueous solution can easily complex with the protons of protonated complex to form renewedly the pyridine ring, which recovers the  $\pi$ -conjugated double-bond system of these fluorophores and hence results in significant fluorescence recovery. According to the deprotonation of nitrogen on the pyridine ring, the fluorescence intensity recovery of all these fluorophores is calculated to be over 75%, implying the excellent reversibility of the fluorescence quenching process. For instance, the emission intensity of fluorophore 2 is calculated to be approximately 76% with the addition of NaOH. These results indicate the reusability of these materials for pH sensing. Such results demonstrated that these fluorophores reveal excellent and reversible pH-sensing photophysical properties, and can be potentially employed as desirable bichromophoric sensor materials for pH sensing.

### 3.4 Fluorescence quenching mechanism

To get an insight into the fluorescence quenching/recovery mechanism, we investigate the absorbance spectral evolution of all these fluorophores under different pH (Fig. 3 and Fig. S27). We find that these fluorophores undergo obvious changes in the

absorbance spectra when varying the pH from neutral to acidic state. The red shift in the absorption spectra of these D-A-D type fluorophores in the presence of hydrogen ions leads to obviously narrowed band gap. Clearly, with the decrease of pH, the strong absorption in the short wavelengths region depletes and new absorption bands arise due to the influence of hydrogen ions (Fig. 3 and Fig. S27). Take fluorophore 5 as an example, with the increase of the acidity, the strong absorption in the visible region (about 432 nm) decrease in the absorbance or even disappear and a new absorption band (centered at around 525 nm) presents. Furthermore, other fluorophores also display similar evolution trends and mechanism in the corresponding absorbance spectra (Fig. S27). We propose the quenching mechanism as follows: with the addition of acids (low pH), protons in the aqueous solution can easily complex with the nitrogen atom of pyridine ring to form the protonated complex, which destroys the  $\pi$ -conjugated double-bond system of these fluorophores and hence results in significant fluorescence quenching.<sup>62</sup> On the other hand, the push-pull effect of D-A type molecules is reduced in acidic conditions.<sup>63</sup>

### 3.5 pH-induced fluorescence sensing of electrosynthesized polymers

According to the molecular-wire effect, D-A-D type conjugated polymers generally exhibit excellent fluorescence and sensing behaviors over their corresponding small molecules.<sup>64-66</sup> All these molecules are supposed to be electropolymerizable due to the terminal thiophene units. Quantum chemistry calculation results also indicate the electropolymerization should occur at the  $\alpha$ -positions of the thiophenes based on to the molecular orbital theory because of higher HOMO portions at these sites (Table 1 and Table S2). To explore the photophysical properties and sensing performances of the conjugated polymers, we successfully electropolymerize these fluorophores in the commonly used electrolytic system DCM-TBAPF<sub>6</sub> (Fig. 4A) The polymerization of these D-A-D type fluorophores happens at  $\alpha$ -positions of end-capping thiophene units (Fig. S23 and Table S1). All these polymers are partially dissolve in common organic solvents, and show significant red-

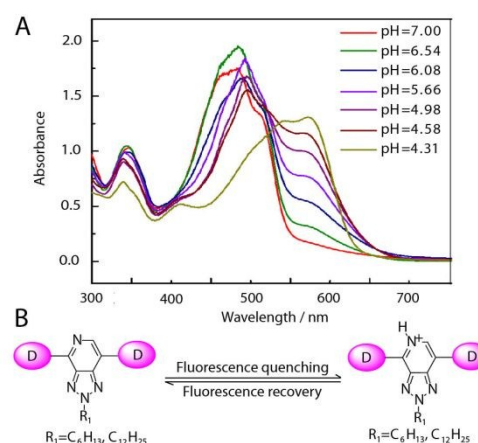


**Fig. 3** (A) The absorbance spectral evolution of fluorophore 5 (15  $\mu$ M) in the pH range of 7.00~4.31. (B) Proposed mechanism of fluorescence quenching for triazolopyridine-thiophene D-A-D type conjugated fluorophores.

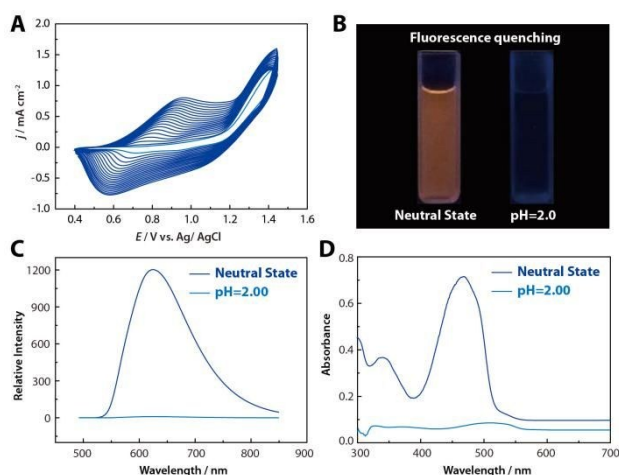


**Fig. 4** (A) Cyclic voltammograms for the electropolymerization of  $0.01 \text{ mol L}^{-1}$  Fluorophore 2 in DCM-TBAPF<sub>6</sub>. Potential scan rate:  $100 \text{ mV s}^{-1}$ . (B) Fluorescence quenching of P2 ( $15 \mu\text{M}$  in repeat units) at the neutral state and pH 2.0. Fluorescence emission (C) and UV-vis absorption (D) spectra of P2 ( $15 \mu\text{M}$  in repeat units) at the neutral state and pH 2.0. Excitation: 380 nm.

shifts in the emission peaks due to the elongation in  $\pi$ -conjugated systems. Unfortunately, compared to their monomeric precursors, they generally display weakened light-emitting nature under 365 nm (Fig. 4 and Fig. S28) probably due to broad molecular weight and compact packing during the electropolymerization. Interestingly, these polymers also display complete fluorescence quenching by adding acids to pH=2.0 (Fig. 4B~D and Fig. S28), demonstrating similar sensing phenomenon and mechanism with their monomeric precursors.

### 3.6 Inkjet-printed complex patterns for practical fluorescent sensing applications

Patterning of conjugated fluorophores into complex geometries is a crucial step for device fabricating and customized requirements. The good solvent processability of these triazolopyridine-thiophene conjugated fluorophores enables us to fabricate stable fluorescent complex solid patterns with advanced manufacturing techniques such as inkjet printing. The fabricated pH test papers and patterns all display effective fluorescence sensing with color changes towards the sensing of acids and even volatile HCl vapor, and can be almost completely recovered by using bases like  $\text{NH}_3 \cdot \text{H}_2\text{O}$  (Fig. 5, Fig. S29, Movie S1, Movie S2). Multiple cyclic fluorescence quenching/recovery tests also indicate very good reversibility of such patterns, which can be advantageous for practical fluorescent sensing applications.<sup>67-72</sup>

## Conclusions

In summary, we successfully synthesized a series of novel triazolopyridine-thiophene D-A-D type conjugated fluorophores by Stille coupling with high yields. These molecules exhibit very high fluorescence quantum yields both in solution (80~89%) and in solid state (13%~26%), and thus

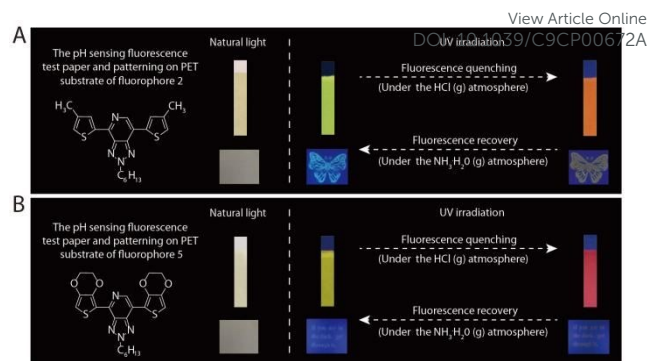


**Fig. 5** Fluorescence test papers and inkjet-printed complex patterns towards effective detection of acids (HCl vapor) and their recovery by bases ( $\text{NH}_3 \cdot \text{H}_2\text{O}$  vapor).

can be employed as excellent fluorescent sensing materials towards practical applications. We further demonstrate that these fluorophores reveal an excellent and reversible pH-induced fluorescence quenching/recovery phenomenon. Enabled by their good processability in common organic solvents, we successfully fabricate sensing devices such as fluorescence papers and complex inkjet-printed patterns for the detection of volatile acids both in solution and vapor atmosphere. Further device fabrication and related applications by combining pH fluorescent sensing behavior and patterning of these molecules are underway in our lab.

## Conflicts of interest

There are no conflicts to declare.

## Acknowledgements

This work was supported by the National Natural Science Foundation of China (51863009, 51763010), Innovation Driven "5511" Project of Jiangxi Province (20165BCB18016), Science Foundation for Excellent Youth Talents in Jiangxi Province (20162BCB23053), the Key Research and Development Program of Jiangxi Province (20171BBH80007, 20181ACB20010), and Science and Technology Foundation of Jiangxi Educational Committee (GJJ160790). K. Q. thanks Jiangxi Educational Committee for a Postgraduate Innovation Program grant (YC2017-S409). N. J. thanks Jiangxi Science & Technology Normal University for a Postgraduate Innovation Program grant (YC2017-X26).

## References

This work was supported by the National Natural Science Foundation of China (51863009, 51763010), Innovation Driven "5511" Project of Jiangxi Province (20165BCB18016), Science Foundation for Excellent Youth Talents in Jiangxi Province (20162BCB23053), the Key Research and Development Program of Jiangxi Province (20171BBH80007, 20181ACB20010), and Science and Technology Foundation of

Jiangxi Educational Committee (GJJ160790). K. Q. thanks Jiangxi Educational Committee for a Postgraduate Innovation Program grant (YC2017-S409). N. J. thanks Jiangxi Science & Technology Normal University for a Postgraduate Innovation Program grant (YC2017-X26).

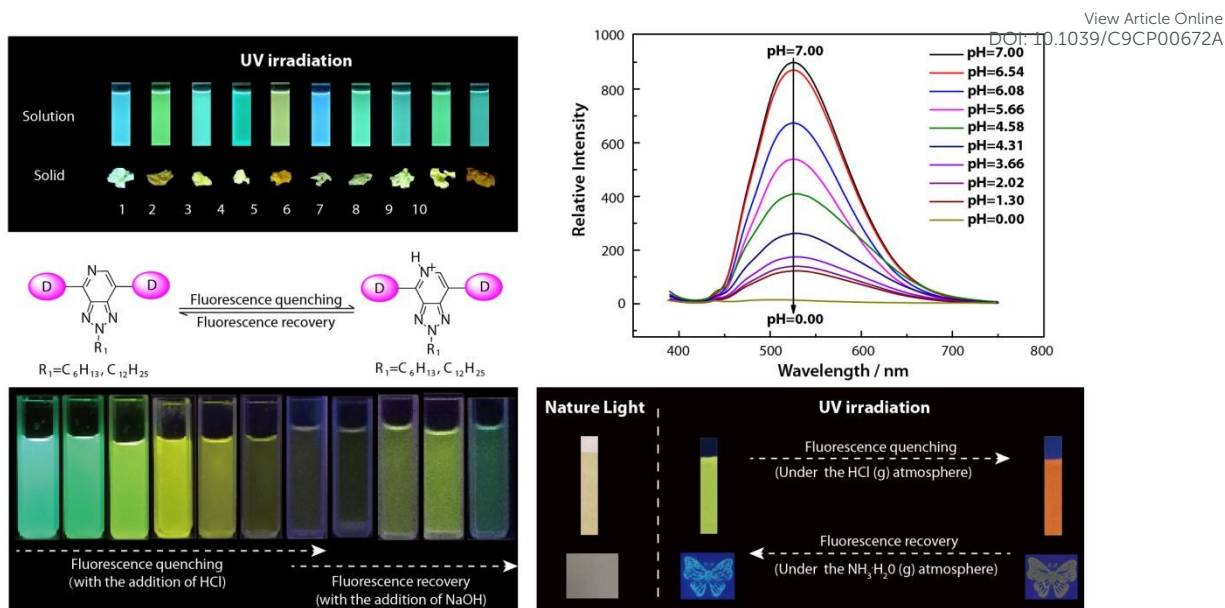
## References

- 1 F. Hu, K. Schmidt-Rohr and M. Hong, *J Am. Chem. Soc.*, 2012, **134**, 3703.
- 2 N. Kang, J.H. Park, K.C. Ko, J. Chun, E. Kim, H.W. Shin, S.M. Lee, H.J. Kim, T.K. Ahn, J.Y. Lee and S.U. Son, *Angew. Chem. Int. Ed.*, 2013, **52**, 6228.
- 3 X.H. Li, X.H. Gao, W. Shi and H.M. Ma, *Chem. Rev.*, 2014, **114**, 590.
- 4 J. Yin, Y. Hu and J. Yoon, *Chem. Soc. Rev.*, 2015, **44**, 4619.
- 5 J.J. Deng, K. Wang, M. Wang, P. Yu and L.Q. Mao, *J Am. Chem. Soc.*, 2017, **139**, 5877.
- 6 I.H. Park, A. Chanthapally, Z.J. Zhang, S.S. Lee, M.J. Zaworotko and J.J. Vittal, *Angew. Chem. Int. Ed.*, 2014, **53**, 414.
- 7 S.Y. Yang, X.L. Deng, R.F. Jin, P. Naumov, M.K. Panda, R.B. Huang, L.S. Zheng and B.K. Teo, *J Am. Chem. Soc.*, 2014, **136**, 558.
- 8 Y. Tang, J.J. Li, Q.F. Guo and G.M. Nie, *Sens. Actuator B Chem.*, 2019, **282**, 824.
- 9 G.M. Nie, Y. Tang, B. Zhang, Y. Wang and Q.F. Guo, *Biosens. Bioelectron.*, 2018, **116**, 60.
- 10 G.M. Nie, Y. Wang, Y. Tang, D. Zhao and Q.F. Guo, *Biosens. Bioelectron.*, 2018, **101**, 123.
- 11 J. Deng, J.F. Li, P.N. Chen, X. Fang, X.M. Sun, Y.S. Jiang, W. Weng, B.J. Wang and H.S. Peng, *J Am. Chem. Soc.*, 2015, **138**, 225.
- 12 J. Deng, Y. Zhang, Y. Zhao, P.N. Chen, X.L. Cheng and H.S. Peng, *Angew. Chem. Int. Ed.*, 2015, **54**, 15419.
- 13 H. Meier, *Angew. Chem. Int. Ed.*, 2005, **44**, 2482.
- 14 P.M. Beaujuge, S. Ellinger and J.R. Reynolds, *Nat. Mater.*, 2008, **7**, 795.
- 15 R. Mukherji, A. Samanta, R. Illathvalappil, S. Chowdhury, A. Prabhune and R.N. Devi, *ACS Appl. Mater. Interfaces*, 2013, **5**, 13076.
- 16 M. Albota, D. Beljonne, J.E. Bredas, J.E. Ehrlich, J.F. Fu, A.A. Heikal, S.E. Hess, T. Kogej, M.D. Levin, S.R. Marder, D. Mccord-Maughon, J.W. Perry, H. Röckel, M. Rumi, G. Subramaniam, W.W. Webb, X.L. Wu and C. Xu, *Science*, 1998, **281**, 1653.
- 17 A. Haldi, A. Kimyonok, B. Domercq and L.E. Scholz, *Adv. Funct. Mater.*, 2008, **18**, 3056.
- 18 M.C. Scharber, M. Koppe, J. Gao, F. Cordella, M.A. Loi, P. Denk, M. Morana, H.J. Egelhaaf, K. Forberich, G. Dennler, R. Gaudiana, G. Waller, Z.G. Zhu, X.B. Shi and C.J. Brabec, *Adv. Mater.*, 2010, **22**, 367.
- 19 Y. Yu, L. Ye, Y.M. Song, Y.D. Guan, J.F. Zang, *Extreme Mech. Lett.*, 2017, **11**, 128.
- 20 Y. Yu, S.L. Jiang, G.Z. Zhang, W.L. Zhou, X.S. Miao, Y.K. Zeng, J. Wang, J.G. He and L. Zhang, *Appl. Phys. Lett.*, 2012, **101**, 073113.
- 21 Q.A. Best, R.S. Xu, M.E. McCarroll, L.C. Wang and D.J. Dyer, *Org. Lett.*, 2010, **12**, 3219.
- 22 S. Kang, S. Kim, Y.K. Yang, S. Bae and J. Tae, *Tetrahedron Lett.*, 2009, **50**, 2010.
- 23 H. Langhals, O. Krotz, K. Polborn and P. Mayer, *Angew. Chem. Int. Ed.*, 2005, **44**, 2427.
- 24 I.D.W. Samuel and G.A. Turnbull, *Chem. Rev.*, 2007, **107**, 1272.
- 25 A.P. De Silva, T.P. Vance, M.E.S. West M.E.S. and G.D. Wright, *Org. Biomol. Chem.*, 2008, **6**, 2468.
- 26 S.L. Ming, S.J. Zhen, K.W. Lin, L. Zhao, J.K. Xu and B.Y. Lu, *ACS Appl. Mater. Interfaces*, 2015, **7**, 11089.
- 27 N.N. Jian, H. Gu, S.M. Zhang, H.T. Liu, K. Qu, S. Chen, X.M. Liu, Y.F. He, G.F. Niu, S.Y. Tai, J. Wang, B.Y. Lu, J.K. Xu and Y. Yu, *Electrochim. Acta*, 2018, **266**, 263.
- 28 B.Y. Lu, S.L. Ming, K.W. Lin, S.J. Zhen, H.T. Liu, H. Gu, S. Chen, Y.Z. Li, Z.Y. Zhu and J.K. Xu, *New J. Chem.*, 2016, **40**, 8316.
- 29 S.L. Ming, S.J. Zhen, X.M. Liu, K.W. Lin, H.T. Liu, Y. Zhao, B. Y. Lu and J.K. Xu, *Polym. Chem.*, 2015, **6**, 8248.
- 30 D. Baran, A. Balan, S. Celebi, B.M. Esteban, H. Neugebauer, N.S. Sariciftci and L. Toppare, *Chem. Mater.*, 2010, **22**, 2978.
- 31 S. Chaurasia, W.I. Hung, H.H. Chou and J.T. Lin, *Org. Lett.*, 2014, **16**, 3052.
- 32 A. Patra, M. Bendikov and S. Chand, *Acc. Chem. Res.*, 2014, **47**, 1465.
- 33 G.L. Gibson, T.M. McCormick and D.S. Seferos, *J Am. Chem. Soc.*, 2012, **134**, 539.
- 34 H. Gu, S.L. Ming, K.W. Lin, S. Chen, X.M. Liu, B.Y. Lu and J.K. Xu, *Electrochim. Acta*, 2018, **260**, 772.
- 35 K.W. Lin, S. Chen, B.Y. Lu, and J.K. Xu, *Sci. China Chem.*, 2017, **60**, 38.
- 36 S.C. Price, A.C. Stuart, L.Q. Yang, H.X. Zhou and W. You, *J Am. Chem. Soc.*, 2011, **133**, 4625.
- 37 W.J. Ying, J.B. Yang, M. Wielopolski, T. Moehl, J.E. Moser, P. Comte, J.L. Hua, S.M. Zakeeruddin, H. Tian and M. Gratzel, *Chem. Sci.*, 2014, **5**, 206.
- 38 Y. Hua, J. He, C.S. Zhang, C.J. Qin, L.Y. Han, J.S. Zhao, T. Chen, W.Y. Wong, W.K. Wong and X.J. Zhu, *J Mater. Chem. A*, 2015, **3**, 3103.
- 39 H.L. Cheng, Z.S. Huang, L.Y. Wang, H. Meler and D.R. Cao, *Dyes Pigm.*, 2017, **13**, 143.
- 40 Y. Sun, S.C. Chien, H.L. Yip, Y. Zhang, K.S. Chen, D.F. Zeigler, D.F. Chen, F.C. Chen, B.P. Lin and A.K.Y. Jen, *J Mater. Chem.*, 2011, **21**, 13247.
- 41 C. Risko, M.D. McGehee and J.L. Bredas, *Chem. Sci.*, 2011, **2**, 1200.
- 42 Z.B. Henson, G.C. Welch, V.D.P. Thomas and C.B. Guillermo, *J. Am. Chem. Soc.*, 2012, **134**, 3766.
- 43 Z.W. Wang, Q. Zhang, K. Zhang and G.K. Hu, *Adv. Mater.*, 2016, **28**, 9857.
- 44 K. Zhang, H.L. Duan, B.L. Karihaloo and J. Wang, *Proc. Natl. Acad. Sci. U. S. A.*, 2010, **107**, 9502.
- 45 T. Lei, J.H. Dou, Z.J. Ma, C.H. Yao, C.J. Liu, J.Y. Wang and J. Pei, *J. Am. Chem. Soc.*, 2012, **134**, 20025.
- 46 X. Zhang, T.T. Steckler, R.R. Dasari, S. Ohira S, W.J. Potscavage Jr, S.P. Tiwari, S. Coppee, S. Ellinger, S. Barlow, J.L. Bredas, B. Kippelen, J.R. Reynolds and S.R. Marder, *J. Mater. Chem.*, 2010, **20**, 123.
- 47 T.T. Steckler, P. Henriksson, S. Mollinger, A. Lundin, A. Salles and M.R. Andersson, *J. Am. Chem. Soc.*, 2014, **136**, 1190.
- 48 D. Aldakov, M.A. Palacios and P. Anzenbacher, *Chem. Mater.*, 2005, **17**, 5238.
- 49 M. Icli-Ozkut, H. Ipek, B. Karabay, A. Cihancer and A.M. Onal, *Polym. Chem.*, 2013, **4**, 2457.
- 50 E.G. Wang, C. Li, W.L. Zhuang, J.B. Peng and Y. Cao, *J Mater. Chem.*, 2008, **18**, 797.
- 51 M.L. Saha, X. Yan and P.J. Stang, *Acc. Chem. Res.*, 2016, **49**, 2527.
- 52 X. Sun, Y. Wang and Y. Lei, *Chem. Soc. Rev.*, 2015, **44**, 8019.
- 53 G. Feng and B. Liu, *Small*, 2016, **12**, 6528.
- 54 Y.F. Wang, T. Zhang and X.J. Liang, *Small*, 2016, **12**, 6451.

## Journal Name ARTICLE

- 55 J. Mei, N.L.C. Leung, R.T.K. Kwok, J.W.Y. Lam and B.Z. Tang, *Chem. Rev.*, 2015, **115**, 11718.
- 56 W.H. Huang, X.P. Zhang, B. Chen, H. Miao, C.O. Trindle, Y.C. Wang, Y. Luo and G.Q. Zhang, *Chem. Comm.*, 2019, **55**, 67.
- 57 J. Peng, W.Q. Yin, J. Shi, X.Y. Jin and G. Ni, *Microchim. Acta*, 2019, **186**, 24.
- 58 G. Meltem, *Biomol. Chem.*, 2019, DOI:10.1021/acs.bioconjchem.8b00861.
- 59 G.C. Welch and G.C. Bazan, *J Am. Chem. Soc.*, 2011, **133**, 4632.
- 60 Y.K. Yang, K.J. Yook and J. Tae, *J Am. Chem. Soc.*, 2005, **127**, 16760.
- 61 L. Prodi, C. Bargossi, M. Montalti, N. Zaccheroni, N. Su, J.S. Bradshaw, R.M. Izatt and P.B. Savage P.B, *J Am. Chem. Soc.*, 2000, **122**, 6769.
- 62 C.G. Niu, X.Q. Gui, G.M. Zeng, A.L. Guan, P.F. Gao and P.Z. Qin, *Anal. Biochem.*, 2005, **383**, 349.
- 63 V.B. Bojinov, N.I. Georgiev and N.V. Marinova, *Sens. Actuator B Chem.*, 2010, **148**, 6.
- 64 A.H. Malik, S. Hussain, A. Kalita and P.K. Iyer, *ACS Appl. Mater. Interfaces*, 2015, **7**, 26968.
- 65 T. Bhuvana, B. Kim, X. Yang, H. Shin and E. Kim, *Angew. Chem. Int. Ed.*, 2013, **52**, 1180.
- 66 S. Seo, C. Allain, J. Na, S. Kim, X. Yang, C. Park, J. Malinge, P. Audebert and K. Kim, *Nanoscale*, 2013, **5**, 7321.
- 67 J. Liu, C. Tan and O. A. Scherman, *Angew. Chem. Int. Eng.*, 2018, **57**, 8854.
- 68 J. Liu and O. A. Scherman, *Adv. Funct. Mater.*, 2018, **28**, 1800848.
- 69 G.Y. Gu, J. Zou, R.K. Zhao, X.H. Zhao and X.Y. Zhu, *Sci. Robot.*, 2018, **3**, 2874.
- 70 G.Y. Gu, U. Gupta, J. Zhu, L.M. Zhu and X.Y. Zhu, *IEEE Trans. Robot.*, 2017, **33**, 1263.
- 71 H. Yuk, B.Y. Lu and X.H. Zhao, *Chem. Soc. Rev.*, 2018, DOI:10.1039/c8cs00595h
- 72 B.Y. Lu, H. Yuk, S.T. Lin, N.N. Jian, K. Qu, J.K. Xu and X.H. Zhao, *Nat. Commun.*, 2019, DOI: 10.1038/s41467-019-09003-5.

View Article Online  
DOI: 10.1039/C9CP00672A



A series of novel triazolopyridine-thiophene D-A-D type conjugated fluorophores are successfully synthesized by Stille coupling with high yields. These fluorophores exhibit very high fluorescence quantum yields both in solution (80~89%) and in solid state (13%~26%), and thus can be employed as excellent fluorescence sensing materials towards practical applications. These fluorophores reveal an excellent and reversible pH-induced fluorescence quenching/recovery phenomenon. Enabled by their good processability in common organic solvents, sensing devices such as fluorescence papers and complex inkjet-printed patterns are successfully fabricated for the detection of volatile acids both in solution and vapor atmosphere.